

The Jensen Effect and Functional Single Index Models: Estimating the Ecological Implications of Nonlinear Reaction Norms

ZI YE¹, GILES HOOKER², STEPHEN ELLNER³

Abstract

This paper develops tools to characterize how species are affected by environmental variability, based on a functional single index model relating a response such as growth rate or survival to environmental conditions. In ecology, the curvature of such responses are used, via Jensen's inequality, to determine whether environmental variability is harmful or beneficial, and differing nonlinear responses to environmental variability can contribute to the coexistence of competing species.

Here, we address estimation and inference for these models with observational data on individual responses to environmental conditions. Because nonparametric estimation of the curvature (second derivative) in a nonparametric functional single index model requires unrealistic sample sizes, we instead focus on directly estimating the effect of the nonlinearity, by comparing the average response to a variable environment with the response at the expected environment, which we call the *Jensen Effect*. We develop a test statistic to assess whether this effect is significantly different from zero. In doing so we re-interpret the SiZer method of Chaudhuri and Marron (1999) by maximizing a test statistic over smoothing parameters. We show that our proposed method works well both in simulations and on real ecological data from the long-term data set described in Drake (2005).

1 Introduction

1.1 Ecological Questions

In natural ecosystems, environmental conditions are highly variable over time and space (e.g., Vasseur and McCann, 2007) and many classical questions in ecology and evolution are therefore

¹PhD Candidate, Department of Statistical Science, Cornell University, zy234@cornell.edu

²Associate Professor, Department of Statistical Science, Cornell University, gjh27@cornell.edu

³Professor, Department of Ecology and Evolutionary Biology, Cornell University, spe2@cornell.edu

concerned with the potential consequences of this variation. Two important topics have been how species' traits and life histories evolve so that species can persist in environments that may be favorable at some times and unfavorable at others (see Cohen (1966) and Koons et al. (2008)). Nonlinear responses to environmental variability can contribute to maintaining the biodiversity of competing species, allowing them to coexist stably (see for example Hutchinson (1961); Chesson and Warner (1981); Ellner (1987); Chesson (1994, 2000b,a)). Nonlinear responses to environmental conditions are also important for forecasting responses to climate change, as environmental variability can either increase population growth rate (Drake (2005); Koons et al. (2009)) or decrease it (Lewontin and Cohen (1969)), depending on the shape of the norm of reaction between environmental variables and the components of population growth rate (survival, growth, and reproduction).

The goal of this paper is to develop methods for determining whether environmental variability is beneficial or harmful for some component of population growth rate, which will depend on whether the response curve is concave-up or concave-down over the range of environmental variability. Common statistical models for species growth and survival make parametric assumptions involving specific forms of nonlinearity, which can pre-determine the effect of environmental variability in the model. For example, in a logistic regression model for survival where the logit(survival) is a linear function of covariates, small variance in one covariate about its mean will increase average survivorship if survival at the mean covariate is below 0.5, and decrease average survivorship if survival at the mean covariate is above 0.5. The conclusion is then driven more by statistical convention than by the data. Recent statistical research in semi-parametric or nonparametric methods inspires us to understand the effect of environmental variation via nonparametric models that do not impose these assumptions. Specifically, we consider spline-based methods (see Wood (2000), Ramsay (2006), Ramsay et al. (2009) and Ruppert et al. (2003)) to predict nonlinear responses under environmental fluctuation.

The nonparametric model considered here is

$$\mathbf{G} = g(\mathbf{E}) + \epsilon, \quad (1)$$

where \mathbf{G} and \mathbf{E} are the growth (or future size) and environment of a plant. The function g is the link function to be estimated, and ϵ is random error. We assume that the environmental \mathbf{E} is

described by a climate history, such as temperature or precipitation observed at a fine time-scale, such as daily resolution. Following Teller et al. (2016), these are thought of as functional covariates, leading to representation of \mathbf{E} as a functional linear term

$$\mathbf{E} = \int X(t) \beta(t) dt, \quad (2)$$

where $\beta(t)$ is the coefficient function to be estimated, and $X(t)$ is the observed climate history.

To assess the impact of variability in \mathbf{E} on the growth rate \mathbf{G} , we need to compare $g[\mathbf{E}(\mathbf{E})]$ (growth under constant conditions) and $\mathbf{E}[g(\mathbf{E})]$. By the Jensen's inequality, we have that $g[\mathbf{E}(\mathbf{E})] \leq \mathbf{E}[g(\mathbf{E})]$ if g is a convex function, and a varying environment will accelerate the growth. Otherwise, if the link function g is concave, a constant environment at the average of environmental factor \mathbf{E} would be more beneficial.

1.2 Model Formulation

Combining (1) and (2), a functional model for observed species growth is

$$Y = g \left(\int X(t) \beta(t) dt \right) + \epsilon. \quad (3)$$

This is the Functional Single Index model introduced in Chen et al. (2011) and Ma (2016). The functional single index model is an extension of the single index model to a functional covariate via $\int X(t) \beta(t) dt$. This model allows a nonlinear relationship between response Y and covariate function $X(t)$. In addition, it improves stability in estimating link function g through imposing smoothness on $\beta(t)$.

To assess the impact of environmental variability, we need to test the convexity or concavity of the link function g . A first approach would be to estimate the curvature of link function g over a domain. We illustrate our estimation procedure in Section 2, where we show that estimating second derivatives requires unrealistic sample sizes.

However, we observed that estimate of the link function g obtained by our procedure is quite accurate. So instead of evaluating the curvature of g , we examine the “Jensen Effect” directly, and estimate the quantity $g[\mathbf{E}(\mathbf{E})] - \mathbf{E}[g(\mathbf{E})]$, or the sign of Jensen's inequality, which only involves an estimate of g . Inspired by the SiZer method Chaudhuri and Marron (1999), we derive a test

based on the maximum estimated value over a range of smoothing parameters. We show that our estimate and hypothesis test work well on both simulated and real data set.

1.3 Related Literature

There is a large literature on the single index model examining both applied methodology and theoretical properties. The link function g and the coefficient vector β have been estimated by three different methods. (1) The most widely used is the Projection Pursuit Regression (PPR) approach introduced in Hardle et al. (1993). This method is a nested estimation procedure, with the link function g estimated by local polynomial approximation and the coefficient function by minimizing the MSE. Theoretical properties were studied in Hardle et al. (1993) and Ichimura (1993). (2) The Average Derivative approach was introduced in Hristache et al. (2001). (3) Li (1991) introduced the Sliced Inverse Regression method, which considered the estimation of the coefficient vector as a dimension-reduction problem.

In contrast, there are few studies of the functional single index model. A counterpart to the Projection Pursuit Regression was introduced in Chen et al. (2011), where the coefficient function β was approximated by a spline basis and the coefficient vector is estimated. In addition, a convergence rate was found for this method. Ma (2016) used two spline bases to approximate the coefficient function and the link function, respectively, and derived some asymptotic properties of the resulting estimate.

The SiZer (SIgnificant ZERo crossings of derivative) method that we adopt to assess significance, introduced in Chaudhuri and Marron (1999), was designed to bypass smoothing parameter selection by comparing the estimates of a curve over a range of smoothing parameters. Our test statistic is inspired by the SiZer method. Instead of trying to select an optimal smoothing parameter for estimation and inference, we examine estimates over a range of smoothing parameters and do inference based on maximizing a test statistic over that range.

2 Estimating Curvature

This section provides a short demonstration of the difficulties of estimating curvature nonparametrically in a functional single index model, which would be necessary for directly using Jensen's inequality to examine the ecological consequences of environmental variability. We first define an estimate for g and discuss some of the numerical challenges it involves, and then provide some results that attempt to estimate g'' directly when selecting smoothing parameters by GCV.

2.1 Estimation Procedure

We consider estimating β , g and g'' via a smoothed basis expansion. Assume that n independent and identically distributed data pairs $(X_1(t), Y_1), \dots, (X_n(t), Y_n)$ are observed where $X_j(t)$ is a real-valued function on $[0,1]$. The Functional Single Index model is

$$Y = g \left(\int X(t) \beta(t) dt \right) + \epsilon$$

where the coefficient function $\beta(t)$ is, like $X(t)$, defined on the interval $[0, 1]$. ϵ is assumed to be Gaussian random error. This integral may need to be evaluated numerically, depending on the representations used for X_i and β , and we assume that this is done up to ignorable error throughout the calculations below. To ensure identifiability of the model, we require that $\int \beta^2(t) dt = 1$.

We use a K_1 -dimensional B-spline basis for the link function g . For any s in the range of possible $\int X\beta$ values, the link function g can be written as

$$g(s) = \phi^\top(s) \mathbf{d},$$

where \mathbf{d} is a K_1 -dimensional column coefficient vector.

We use a K_2 -dimensional Fourier basis for the coefficient function β , such that

$$\beta(t) = \psi^\top(t) \mathbf{c},$$

where \mathbf{c} is a K_2 -dimensional column coefficient vector, and $t \in [0, 1]$. The constraint $\|\beta\| = 1$ is reduced to requiring $\|\mathbf{c}\| = 1$ in this case.

The coefficient vectors \mathbf{c} and \mathbf{d} are estimated by minimizing a penalized sum of squares

$$\begin{aligned} \text{2PLS} &\doteq \sum_{i=1}^n (Y_i - g_i)^2 + \lambda_g \int \left(g^{(2)}(s) \right)^2 ds + \lambda_\beta \int \left(\beta^{(2)}(t) \right)^2 dt \\ &= \sum_{i=1}^n \left\{ Y_i - \boldsymbol{\phi}^\top \left[\left(\int X_i \boldsymbol{\psi}^\top \right) \mathbf{c} \right] \mathbf{d} \right\}^2 + \lambda_g \mathbf{d}^\top \mathbb{P}_g \mathbf{d} + \lambda_\beta \mathbf{c}^\top \mathbb{P}_\beta \mathbf{c}, \end{aligned} \quad (4)$$

where $g_i \doteq g \left(\int X_i \beta \right)$ and the penalty matrices $[\mathbb{P}_\beta]_{ij} = \int \psi_i^{(2)}(t) \psi_j^{(2)}(t) dt$ and $[\mathbb{P}_g]_{ij} = \int \phi_i^{(2)}(t) \phi_j^{(2)}(t) dt$ are available analytically for most common choices of basis expansion.

Equation (4) specifies a nonlinear optimization problem, which we solve numerically using built-in optimizers in R (see below). Denoting the estimated coefficients as $\hat{\mathbf{c}}$ and $\hat{\mathbf{d}}$, the estimates are

$$\hat{\beta}(t) = \boldsymbol{\psi}^\top(t) \hat{\mathbf{c}},$$

and

$$\hat{g}_i \doteq \hat{g} \left(\int X_i \hat{\beta} \right) = \boldsymbol{\phi}^\top \left[\left(\int X_i(t) \boldsymbol{\psi}^\top(t) dt \right) \hat{\mathbf{c}} \right] \hat{\mathbf{d}},$$

where $i = 1, \dots, n$.

2.2 Bases, Optimization and Cross-Validation

Our objective criterion (4) requires nonlinear numerical optimization. In our experiments below we have used the R function `optim` with some additional modifications. The simulations reported in Section 4 used the BFGS gradient-based optimizer. However, at large values of λ we find that very tight convergence criteria are needed to reduce the numerical error below that of the estimated noise. This was mitigated with two strategies:

1. We initialize our optimization with \mathbf{d} chosen so that \hat{g} is exactly linear and \mathbf{c} is obtained from functional linear regression.
2. We re-initialize BFGS once it converges, and run it a second time. BFGS uses a sequentially-calculated approximate Hessian, and can stop early due to poor estimation of this Hessian. Re-initialization resets the approximate Hessian to the identity, so that optimization is restarted with a steepest descent step.

To maintain identifiability of our model, we normalize our estimate of $\beta(t)$ within each evaluation of the objective function and multiply by $\text{sign}(\beta(0))$.

In order to represent \hat{g} with a basis expansion, we need to control the range of its arguments. Throughout our estimates below, we have used the identifiability requirement that $\|\beta\| = 1$ to use a range of $[-S, S]$ where S is the largest score for the maximum eigenvalue from a principal components decomposition of the X_i . If $|\int X_i(t)\beta(t)dt| > S$ we replace the argument with the corresponding end-point of the range and add a penalty of $|\int X_i(t)\beta(t)dt| - S$ to the objective (4). In practice, while we find that this exceedence can occur during optimization, it never appears in the final result.

To illustrate the impact of initial conditions on our estimates, as well as the challenge of estimating curvature in functional single index models, Section 2.3 below presents examples of estimating g'' with initial conditions either given by the true basis coefficients \mathbf{c} and \mathbf{d} or by starting from $\mathbf{c} = \left(\frac{1}{\sqrt{K_2}}, \dots, \frac{1}{\sqrt{K_2}}\right)$, using Nelder-Mead optimization. In each case, different initialization procedures yield quite different performance statistics, but all perform poorly in estimating curvature.

While our assessment of statistical significance avoids selecting λ , it will be useful to have a value for visualization and for an estimate of residual variance. To choose λ , we define a smoother matrix \mathbb{S}_λ associated with λ , and the GCV value for selecting λ is calculated from

$$\text{GCV}(\lambda) \doteq \frac{\frac{1}{n} \|(\mathbb{I} - \mathbb{S}(\lambda)) \mathbf{Y}\|^2}{\left[\frac{1}{n} \text{tr}(\mathbb{I} - \mathbb{S}(\lambda))\right]^2},$$

where \mathbb{I} is the $(n \times n)$ -dimensional identity matrix. We derive \mathbb{S}_λ from a Taylor expansion in (5) below.

2.3 A Simulated Demonstration

We present here a brief simulation study to observe the accuracy of curvature estimates. The covariate function $X(t)$ was generated based on a Fourier basis

$$X_i(t) = \mu(t) + \sum_{k=1}^4 \xi_{ik} \eta_k(t), \quad i = 1, \dots, n,$$

where $\mu(t) = t$, $\eta_1(t) = \frac{1}{\sqrt{2}} \sin(2\pi t)$, $\eta_2(t) = \frac{1}{\sqrt{2}} \cos(2\pi t)$, $\eta_3(t) = \frac{1}{\sqrt{2}} \sin(4\pi t)$, $\eta_4(t) = \frac{1}{\sqrt{2}} \cos(4\pi t)$, and ξ_{ik} are i.i.d $N(0, \gamma_k)$ with $\gamma_1 = 1$, $\gamma_2 = \frac{1}{2}$, $\gamma_3 = \frac{1}{4}$, $\gamma_4 = \frac{1}{8}$. The coefficient function is

$$\beta(t) = 2 \left[\frac{1}{\sqrt{12}} \eta_1(t) + \frac{1}{\sqrt{12}} \eta_2(t) + \frac{1}{\sqrt{6}} \eta_3(t) + \frac{1}{\sqrt{6}} \eta_4(t) \right].$$

We observe that the coefficients for β satisfy $\|\beta\| = 1$, under an orthonormal basis. The random errors ϵ_i are simulated as i.i.d. Gaussian noise with mean 0 and $\text{var}(\epsilon) = 0.1 \text{var}[g(\int X\beta)]$.

We selected the sample size as $n = 100$ and examined three link functions:

1. $g(s) = e^{-s}$.
2. $g(s) = -s^2$.
3. $g(s) = s$.

To measure the performance of our estimators we define the MSE of the estimated β and $g^{(k)}$ to be

$$\text{RSE} = \left[\int (\hat{\beta}(t) - \beta(t))^2 dt \right]^{\frac{1}{2}},$$

and

$$\text{RASE}(k) = \left\{ \frac{1}{n} \sum_{i=1}^n \left[\hat{Y}_i^{(k)} - g^{(k)} \left(\int X_i(t) \beta(t) dt \right) \right]^2 \right\}^{\frac{1}{2}},$$

where $\hat{Y}_i^{(k)} = \hat{g}^{(k)} \left(\int X_i(t) \hat{\beta}(t) dt \right)$ for $k = 0, 1, \dots$.

Of particular concern in the results (Table 1) is the substantial discrepancy between estimates from different initial conditions. Ye and Hooker (2018) similarly observed that second derivative estimates were highly sensitive to the effort placed into optimization.

Initial	g1			g2			g3		
	RSE	RASE	RASE2	RSE	RASE	RASE2	RSE	RASE	RASE2
True	1.1213	0.0921	5.2517	0.5385	0.0490	2.9079	0.7608	0.0706	5.4393
Equal	0.6417	0.0800	3.0516	0.6980	0.0730	4.1328	0.7024	0.0764	1.2170

Table 1: Simulation results with $(\lambda_g, \lambda_\beta)$ selected by GCV. Values in the Table are averages over 100 simulations.

The plots in Figure 1 provide an example of our results. The estimate of the link function nearly overlaps the true curve, indicating that our estimate of the link function is quite accurate. However, for the second derivative, the estimate deviates from the true curve, in fact becoming negative towards the right-hand limit. This reduced accuracy is also evident in the results in Table 1. These plots indicate that our estimate of the curvature is not good enough to use as a basic for decisions on the convexity of g . In addition, the performance of the estimators varies a lot from different initial values. In Figure 2 we see that different initial conditions can lead to either over- or under-fitting g'' . Further examples are provided in Appendix A. We therefore directly assess the Jensen Effect via other methods, introduced in the next section.

3 Jensen Effect

The ecological interest in g'' is in the comparison of $g[\mathbf{E}(\mathbf{E})]$ and $\mathbf{E}[g(\mathbf{E})]$. Because reliable estimate of g'' requires unrealistic sample sizes, we instead compare these quantities directly to estimate what we call the “Jensen Effect”.

We define a difference statistic by

$$\delta = \frac{1}{n} \sum_{i=1}^n g\left(\int X_i \beta\right) - g\left(\int \bar{X} \beta\right),$$

where $\bar{X} = \frac{1}{n} \sum_{i=1}^n X_i$. If the link function g is convex, then $\delta > 0$ which indicates better growth with a varying environment; otherwise, the difference $\delta < 0$ and a constant environment is better for growth. However, this estimate still depends on the smoothing parameters λ_g and λ_β .

To account for the choice of smoothing parameters, we extend the SiZer method, first introduced for local linear regression in Chaudhuri and Marron (1999), and then extended to smoothing splines setting in Marron and Zhang (2005). SiZer is a graphical tool to make inference about features on an estimated curve, and detect features of that curve in an innovative way. Traditional nonparametric methods have difficulties in selecting a appropriate bandwidth in a local linear approximation, or a smoothing parameter in a smoothing spline. Classical methods such that 10-fold cross-validation and generalized cross-validation provide point estimates, but it is difficult to incorporate their uncertainty into inference about the resulting curves. The SiZer method skips the process of

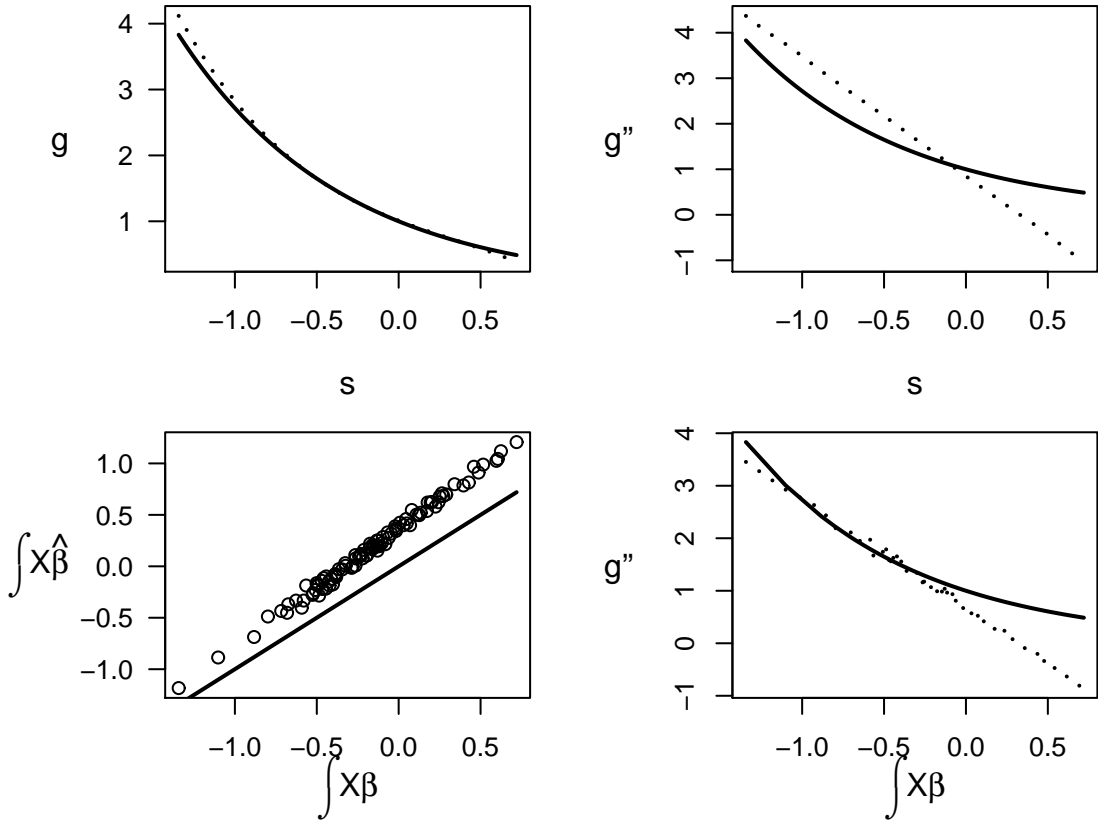


Figure 1: Example estimate for the link function $g(s) = e^{-s}$. Top-left and right panels plot g and g'' over 1000 equally-spaced grid points between the minimum and maximum of $\int X(t) \hat{\beta}(t) dt$. Dots are estimated values, and the solid curves are the truth. The bottom-left panel plots $\int X(t) \hat{\beta}(t) dt$ versus $\int X(t) \beta(t) dt$ (circles); the solid line is the 1:1 line. The bottom-right panel presents g'' (black) and \hat{g}'' (red) evaluated at $\int X(t) \beta(t) dt$ and $\int X(t) \hat{\beta}(t) dt$ respectively but plotted against the true argument.

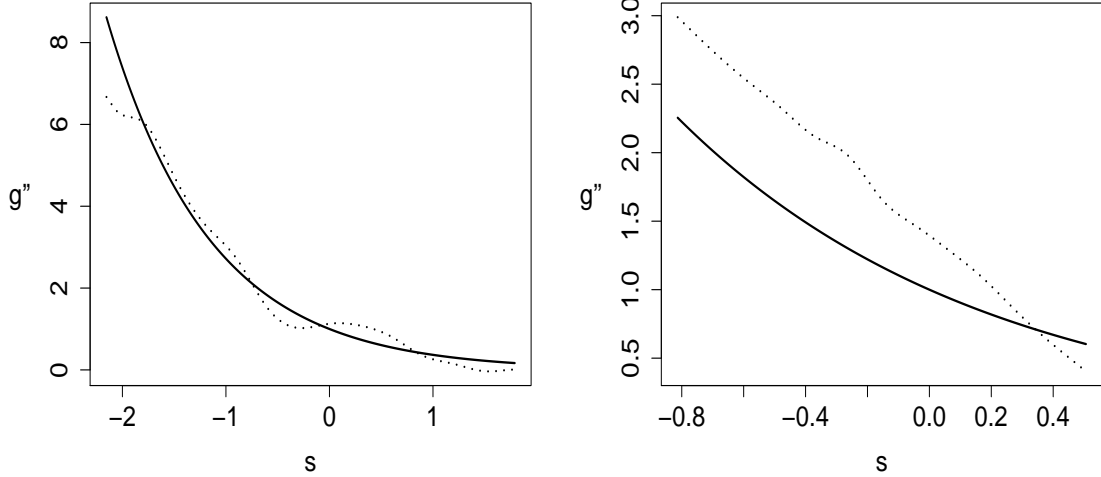


Figure 2: Estimates for g'' from different initial conditions. Left, using the known true g as the initial condition. Right, starting from equal values of the coefficients. Note that this example was chosen for illustrative purposes and does not use the same data as Figure 1.

selecting a tuning parameter. Instead, it examines the estimate of a curve over a range of tuning parameters, and observes features of the curve for each combination of observation point and tuning parameter. Inspired by the SiZer method, we look the difference δ over a range of λ values for g and β , and generate hypothesis tests using the maximum or minimum value of δ as a function of λ .

3.1 Hypothesis Test 1: Nonparametric Smoothing

We begin by briefly developing our SiZer-inspired test for a standard smoothing spline (treating the environment E as known) before developing the test for a functional single index model. Here defining Φ to be matrix of evaluations, $\Phi_{ij} = \phi_j(E_i)$ and \mathbb{P} to be the second derivative penalty matrix, the standard smoothing spline estimate is

$$\hat{g}_\lambda(e) = \phi(e)^T (\Phi^T \Phi + \lambda \mathbb{P})^{-1} \Phi^T \mathbf{Y}.$$

Define the $(n+1)$ -dimensional column vector $\mathbf{a} = (\frac{1}{n}, \dots, \frac{1}{n}, -1)^\top$ and the augmented set of evaluation points $\mathbf{e} = (E_1, \dots, E_n, \bar{E})$ with corresponding evaluation matrix Φ^+ . We can write

$$\delta_\lambda = \frac{1}{n} \sum \hat{g}_\lambda(E_i) - \hat{g}_\lambda(\bar{E}) = \mathbf{a}^T \Phi^+ (\Phi^T \Phi + \lambda \mathbb{P})^{-1} \Phi^T \mathbf{Y} = \mathbf{u}_\lambda \mathbf{Y}$$

which we can standardize to obtain the t -statistic

$$t_\lambda = \frac{\mathbf{u}_\lambda \mathbf{Y}}{\sigma \sqrt{\mathbf{u}_\lambda \mathbf{u}_\lambda^T}}.$$

We treat the value of t_λ as a Gaussian process over λ with covariance function

$$\Sigma(\lambda_1, \lambda_2) = \frac{\mathbf{u}_{\lambda_1} \mathbf{u}_{\lambda_2}}{\|\mathbf{u}_{\lambda_1}\| \|\mathbf{u}_{\lambda_2}\|}$$

which involves no unknown parameters. We can thus use $\max_\lambda |t_\lambda|$ as a test statistic, obtaining critical values by simulating from the Gaussian process $\mathbb{GP}(\mathbf{0}, \Sigma)$. In practice, we need to estimate $\hat{\sigma}$ which we do based on the value λ selected by GCV.

An important consideration here is that we expect δ_λ to inherit smoothing bias, but this should result in under-estimation of the Jensen Effect because it will shrink the estimated second derivative. By examining t_λ over the whole range of λ we can assess this effect at various levels of smoothing while maintaining a conservative test. We do still need to choose λ by GCV in our estimate $\hat{\sigma}^2$. We expect $\hat{\sigma}^2$ to be relatively insensitive to the specific λ chosen; maintaining a constant $\hat{\sigma}^2$ in the t -statistic removes the need to account for changes in $\hat{\sigma}^2$ across λ .

3.2 Hypothesis Test 2: Functional Single Index Models

The functional single index model complicates the process described above by including two smoothing parameters and nonlinear effects of $\hat{\beta}$, necessitating a Taylor expansion to approximate the recipe above. For each pair of smoothing parameters $(\lambda_g, \lambda_\beta)$, we obtain an estimate of β , g , and δ , denoted as $\hat{\delta}(\lambda_g, \lambda_\beta)$. Defining

$$\begin{aligned} \mathbf{i} &= \left(\int X_1 \hat{\beta}, \dots, \int X_n \hat{\beta}, \int \bar{X} \hat{\beta} \right)^\top, \\ \mathbf{i}_{-1} &= \left(\int X_1 \hat{\beta}, \dots, \int X_n \hat{\beta} \right)^\top, \\ \mathbf{v} &= \left(\hat{g} \left(\int X_1 \hat{\beta} \right), \dots, \hat{g} \left(\int X_n \hat{\beta} \right), \hat{g} \left(\int \bar{X} \hat{\beta} \right) \right)^\top, \end{aligned}$$

the estimated difference function given $(\lambda_g, \lambda_\beta)$ is

$$\begin{aligned}\hat{\delta}(\lambda_g, \lambda_\beta) &= \mathbf{a}^\top \mathbf{v} = \mathbf{a}^\top \boldsymbol{\phi}(\mathbf{i}) \hat{\mathbf{d}} \\ &= \mathbf{a}^\top \boldsymbol{\phi}(\mathbf{i}) \left(\boldsymbol{\phi}(\mathbf{i}_{-1})^\top \boldsymbol{\phi}(\mathbf{i}_{-1}) + \lambda_g \mathbb{P}_g \right)^{-1} \boldsymbol{\phi}(\mathbf{i}_{-1})^\top \mathbf{Y}.\end{aligned}$$

To construct a t-statistic to test the significance of δ , an estimate of the variance of the difference function δ is needed. The estimated difference function $\hat{\delta}(\lambda_g, \lambda_\beta)$ is defined on an estimate of $\hat{\mathbf{c}}$ and $\hat{\mathbf{d}}$, which are the coefficients of β and g respectively. Therefore, we need to calculate the covariance of the estimated $\hat{\mathbf{c}}$ and $\hat{\mathbf{d}}$.

Recall (4), the penalized least squares criterion to be minimized, and define the matrices of linear basis effects $\Psi_{ij} = \int X_i(t) \psi_j(t) dt$ and evaluations of the link function bases and derivatives $\Phi_{ij}^{(k)} = \phi_j^{(k)}(\Psi_{i\cdot} \mathbf{c})$ with \mathbf{c} taken at its expected estimate. We derive gradients of PLS as

$$\begin{pmatrix} \nabla \mathbf{d} \\ \nabla \mathbf{c} \end{pmatrix} = \begin{pmatrix} \Phi^\top \{\mathbf{Y} - \Phi \mathbf{d}\} + \lambda_g \mathbb{P}_g \mathbf{d} \\ \Psi^\top \text{diag}\{\Phi^{(1)} \mathbf{d}\} \{\mathbf{Y} - \Phi^\top \mathbf{d}\} + \lambda_\beta \mathbb{P}_\beta \mathbf{c} \end{pmatrix} = \begin{pmatrix} \mathbb{Z}_g \\ \mathbb{Z}_\beta \end{pmatrix} (\mathbf{Y} - \Phi \mathbf{d}) + \begin{pmatrix} \lambda_g \mathbb{P}_g \mathbf{d} \\ \lambda_\beta \mathbb{P}_\beta \mathbf{c} \end{pmatrix}$$

and expected Hessian

$$\mathbb{H} = \begin{pmatrix} \mathbb{Z}_g^T \mathbb{Z}_g + \lambda_g \mathbb{P}_g & \mathbb{Z}_g^T \mathbb{Z}_\beta \\ \mathbb{Z}_\beta^T \mathbb{Z}_g & \mathbb{Z}_\beta^T \mathbb{Z}_\beta + \lambda_\beta \mathbb{P}_\beta \end{pmatrix}.$$

We can now obtain the sandwich covariance

$$\text{cov} \begin{pmatrix} \mathbf{d} \\ \mathbf{c} \end{pmatrix} = \hat{\sigma}^2 \mathbb{H}^{-1} \begin{pmatrix} \mathbb{Z}_g \\ \mathbb{Z}_\beta \end{pmatrix}^\top \begin{pmatrix} \mathbb{Z}_g \\ \mathbb{Z}_\beta \end{pmatrix} \mathbb{H}^{-1}$$

where we estimate σ^2 from

$$\hat{\sigma}^2 = \frac{1}{\text{df}_{\text{res}}} \sum_{i=1}^n \left[Y_i - \hat{g} \left(\int_0^1 X_i \hat{\beta} \right) \right]^2.$$

As in Ruppert et al. (2003), the residual degree of freedom is defined as

$$\text{df}_{\text{res}} = n - 2\text{tr}(\mathbb{S}) + \text{tr}(\mathbb{S} \mathbb{S}^\top) - K_1,$$

where

$$\mathbb{S} \doteq \mathbb{S}(\lambda_g, \lambda_\beta) = \begin{pmatrix} \mathbb{Z}_g \\ \mathbb{Z}_\beta \end{pmatrix} \mathbb{H} \left(\mathbb{Z}_g^\top, \mathbb{Z}_\beta^\top \right) \quad (5)$$

is an approximate smoother matrix in which we use the values of $(\lambda_g, \lambda_\beta)$ selected by GCV.

We now define a t-statistic for δ as a function of λ ,

$$t \doteq t(\lambda_g, \lambda_\beta) \doteq \frac{\hat{\delta}(\lambda_g, \lambda_\beta)}{\text{sd}[\hat{\delta}(\lambda_g, \lambda_\beta)]}.$$

where $\text{sd}[\hat{\delta}(\lambda_g, \lambda_\beta)]$ is given by

$$\text{sd}[\hat{\delta}(\lambda_g, \lambda_\beta)] = \left\{ [\mathbf{a}^\top \phi(\mathbf{i})] \text{cov}(\hat{\mathbf{d}}) [\mathbf{a}^\top \phi(\mathbf{i})]^\top \right\}^{\frac{1}{2}}.$$

Defining the n -dimensional row vector \mathbf{u}_λ as

$$\mathbf{u}_\lambda = \mathbf{a}^\top \phi(\mathbf{i}) \left(\phi(\mathbf{i}_{-1})^\top \phi(\mathbf{i}_{-1}) + \lambda \mathbb{P} \right)^{-1} \phi(\mathbf{i}_{-1})^\top,$$

the estimated covariance matrix of $\hat{\delta}_\lambda$ is $\hat{\sigma}^2 \mathbf{u}_\lambda \mathbf{u}_\lambda^\top$. δ_λ is therefore approximately a Gaussian process indexed by λ and we can get the estimated variance of t_λ from $\frac{\mathbf{u}_\lambda \mathbf{u}_\lambda^\top}{\|\mathbf{u}_\lambda\|^2}$.

We want to test if $\delta \equiv 0$. Denote the number of the smoothing parameters λ_g as m , we test H_0 : $(\hat{\delta}_{\lambda_1}, \dots, \hat{\delta}_{\lambda_m})^\top = \mathbf{0}_m$. Under H_0 , $(t_{\lambda_1}, \dots, t_{\lambda_m})^\top \sim N(\mathbf{0}_m, \mathbb{A}_{mm})$, where $\mathbf{0}_m$ is a m -dimensional column vector, and the covariance matrix \mathbb{A} is $(m \times m)$ -dimensional with the (i, j) term equals to $\frac{\mathbf{u}_{\lambda_i} \mathbf{u}_{\lambda_j}^\top}{\|\mathbf{u}_{\lambda_i}\| \|\mathbf{u}_{\lambda_j}\|}$. The test statistic that we examine is $T = \max \{t_{\lambda_1}, \dots, t_{\lambda_m}\}$.

In order to obtain a critical value for this statistic, we repeatedly simulate t_λ from $N(\mathbf{0}_m, \mathbb{A}_{mm})$ and obtain a distribution for $\max_\lambda |t_\lambda|$.

4 Simulation Study

In this section, we use simulated data to explore the power of our test for both single index and functional single index models.

4.1 Single Index Model

We test for a Jensen Effect by calculating the difference function δ over a range of smoothing parameters. If the link function g is convex, the δ function will be positive for most of λ values, although it may have high variance at low λ and high bias at high λ . For each simulation, we conduct the hypothesis test introduced in previous section.

Our simulation study starts with the single index model with $p = 5$ covariates generated uniformly on $[-0.5, 0.5]$, and the coefficient $\beta = \frac{1}{\sqrt{p}}\mathbf{1}_p$ so that $\|\beta\| = 1$.

To illustrate the Jensen Effect, we choose three different link functions, (1) $g(s) = e^s$, (2) $g(s) = -s^2$, (3) $g(s) = s$. We represented g by a 25-dimensional quintic B-spline basis. For each link function, we simulated 1000 data sets of size 100, with error standard deviation 0.1. We obtained critical values for our test by simulating 5000 normal samples from the null distribution. Figure 3 presents a sample of δ_λ and t_λ functions functions versus $\log(\lambda)$ for $g(s) = e^s$; plots for the other link functions are in Appendix B. The rejection rates for these functions are: 99.2%, 99.3% and 5.7% respectively.

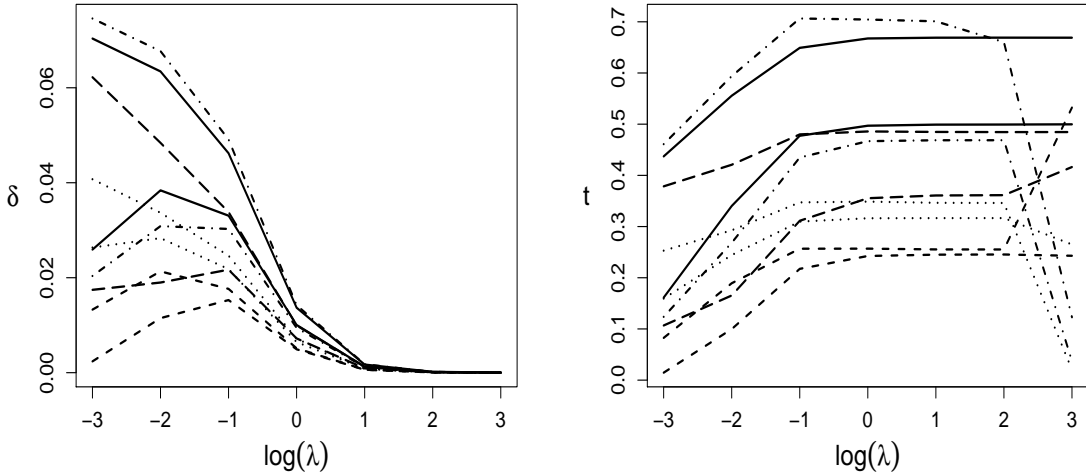


Figure 3: Left: a sample of δ_λ as a function of λ in a single index model with link function $g(s) = e^s$. Right: the corresponding t_λ functions.

4.2 Functional Single Index Model

To define a distribution for the functional covariates, we use a 25-dimensional Fourier basis $\psi(t)$, where $t \in [0, 1]$. The covariate functions $X(t)$ are generated as

$$X(t) = \sum_{i=1}^{25} \xi_i \psi_i(t),$$

where $\xi_i = N(0, e^{-(i-1)/12})$. The coefficient function is

$$\beta(t) = \mathbf{c}^\top \psi(t),$$

where $\mathbf{c} = (0, 1, 1, 0.5, 0, \dots, 0)^\top$.

Again we used the three link functions $g(s) = e^s$, $g(s) = -s^2$, $g(s) = s$. We represented g by a 25-dimensional quintic B-spline basis. For each link function, we generated 1000 simulated data sets of size 100 with error standard deviation 0.1, and for each such data set we generated 5000 normal samples from the null distribution to obtain critical values.

A plot of the δ_λ and t_λ functions for $g(s) = e^s$ is presented in Figure 4. We have placed equivalent plots for $g(s) = -s^2$ and $g(s) = s$ in Appendix C. The rejection rates for the three link functions were 100%, 100% and 7.3%, showing very good power with a reasonable sample size and close to nominal rate when the null hypothesis is true (no curvature).

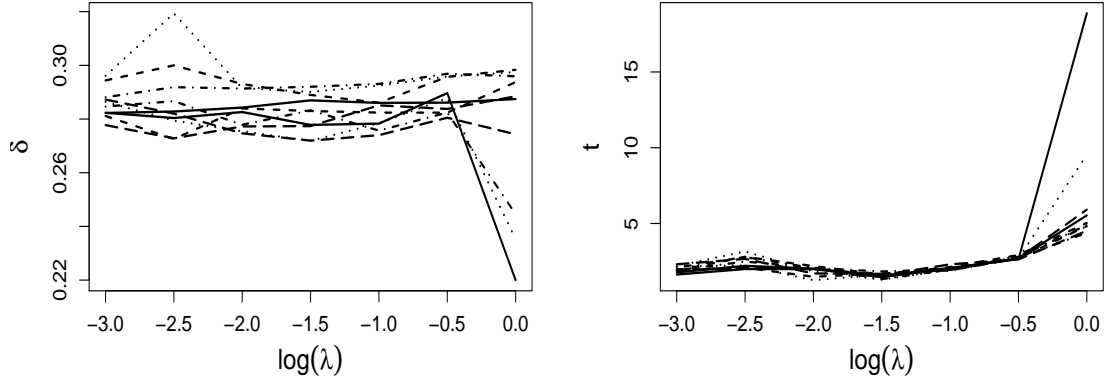


Figure 4: Left: a sample of δ_λ as a function of λ in a functional single index model with link function $g(s) = e^s$. Right: the corresponding t_λ functions.

4.3 Power Analysis

To investigate the power of our test in more detail we consider a series of increasingly nonlinear link functions

$$g(s) = s + \eta e^{-s},$$

with $0 \leq \eta \leq 1.2$ for the single index model and $0 \leq \eta \leq 0.8$ for the functional single index model. As η increases, g becomes strongly convex. For each η , we generate 1000 simulated data sets and again used 5000 normal samples under the null distribution to obtain critical values.

Figure 5 presents the rejection rate plotted against η . We observe a sharp increase as η increases, as expected. As the link function g becomes more and more convex, the rejection rate will converge to 1.

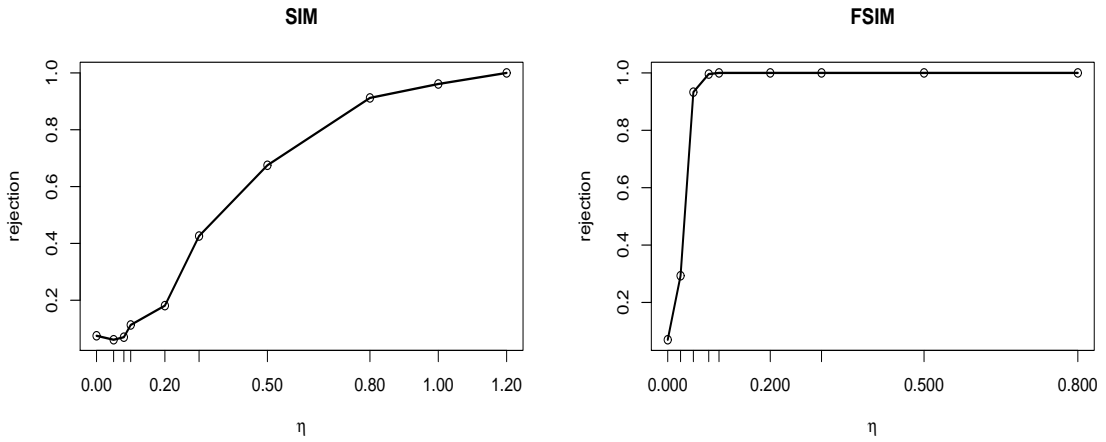


Figure 5: The power function of the Jensen Effect test plotted against η in the link function $g(s) = s + \eta e^{-s}$. A single index model using the simulation settings from Section 4.1 produced the left plot, while the right-hand plot is obtained using a functional single index model with settings described in Section 4.2.

5 Application to real ecological data

To demonstrate application of our tests, we analyze the North Temperate Lakes LTER: Zooplankton - Trout Lake Area data set (<https://portal.edirepository.org/nis/mapbrowse?scope=knb-lter-ntl&identifier=37&rev=1>). An earlier version of these data were analyzed by Drake (2005) to examine the temperature-dependence of copepod populations. In our data set, the density of the populations of nine species of copepods and rotifers, along with water temperature, were recorded from 1981 to 2015 in 8 different lakes. Our choice of species was determined based on the number and length of observations available and differs from those studied in Drake (2005). Note that the growth response in these data is not the growth (in size) of an individual, but the growth (in numbers) of a population, but our functional single index model is still appropriate for this setting.

The values recorded in the original data set are:

1. d : species' density at a specific time and lake.
2. t : record of temperature corresponding to the same time as d . The temperature was recorded on irregular time points among different years and lakes, so we pre-processed the temperature data by fitting a smoothing spline.

At the time of each observed response, we used lake temperature values over the 60 preceding days as the climate history covariate $X(t)$. For each lake, we fit a penalized spline functional single index model for the growth in population density as a function of temperature history in each lake. We used 37 fourier Basis functions to represent $\beta(t)$ in each case and a 21-dimensional cubic B-spline basis to represent g , and searched over values of $\log(\lambda)$ from 10^{-6} to 10^6 .

The p -values for 9 species are given in Table 2; plots of the estimates of g , g'' and δ functions are given in Appendix D. *Kellicottia longispina* and *Polyarthra remata* have significantly nonzero Jensen effects ($p < 0.05$), indicating evidence of nonlinear responses by those species. The δ function of these two species are different from 0 over the prespecified range of smoothing parameters. In the plots of the δ function of these two species, we observe that their δ functions are above zero over the range of λ , showing that their link functions are convex. Thus, their average growth rate is increased by the presence of environmental variation.

Species	Sample Size	p-value
<i>Diacyclops thomasi</i>	1482	0.170
<i>Filinia terminalis</i>	461	0.512
<i>Gastropus stylifer</i>	1083	0.140
<i>Kellicottia longispina</i>	1541	0.014*
<i>Keratella cochlearis</i>	1654	0.726
<i>Keratella earlinae</i>	1092	0.425
<i>Keratella quadrata</i>	689	0.059
<i>Polyarthra remata</i>	1553	0.003*
<i>Polyarthra vulgaris</i>	1771	0.338

Table 2: Sample size and p -value for each species in LTER dataset. * indicates that the p -value is significant for the hypothesis test at level $\alpha = 0.05$.

6 Conclusion

To determine whether a species' growth rate is increased or decreased by environmental variability, we examine the Jensen Effect. Our first attempt in this direction was to estimate the curvature of the link function in a Functional Single Index model. In our penalized spline based method, we found that unrealistic sample size was needed to obtain accurate estimates. So instead we investigated the net effect of Jensen's inequality, by comparing the expected response (averaged across the environmental variation) to the response at the expected environment. Inspired by the SiZer method, our test is based on maximizing across a wide range encompassing all plausible smoothing parameter values, thus avoiding the need for smoothing parameter selection. We have shown that our method and test work well on both simulated and real data.

There are multiple potential extensions of this methodology. We have used observed data as representative of the covariates of interest. However, the test can be conducted for any assumed distribution of covariates and it may be of interest to describe regions of single index values in

which the estimated link function exhibits Jensen’s Inequality. We have also applied this model to growth data, using least-squares. For survival data all standard link functions impose particular curvature structures. These can be modified by adding a nonparametric function within the link, but obtaining equivalent tests – since the relevant effect is on survival itself, not its logit-transform – requires further development.

References

Chaudhuri, P. and J. S. Marron (1999). Sizer for exploration of structures in curves. *Journal of the American Statistical Association* 94(447), 807–823.

Chen, D., P. Hall, H.-G. Müller, et al. (2011). Single and multiple index functional regression models with nonparametric link. *The Annals of Statistics* 39(3), 1720–1747.

Chesson, P. (1994). Multispecies competition in variable environments. *Theoretical population biology* 45(3), 227–276.

Chesson, P. (2000a). General theory of competitive coexistence in spatially-varying environments. *Theoretical population biology* 58(3), 211–237.

Chesson, P. (2000b). Mechanisms of maintenance of species diversity. *Annual review of Ecology and Systematics* 31(1), 343–366.

Chesson, P. L. and R. R. Warner (1981). Environmental variability promotes coexistence in lottery competitive systems. *The American Naturalist* 117(6), 923–943.

Cohen, D. (1966). Optimizing reproduction in a randomly varying environment. *Journal of theoretical biology* 12(1), 119–129.

Drake, J. M. (2005). Population effects of increased climate variation. *Proceedings of the Royal Society of London B: Biological Sciences* 272(1574), 1823–1827.

Ellner, S. (1987). Alternate plant life history strategies and coexistence in randomly varying environments. In *Theory and models in vegetation science*, pp. 199–208. Springer.

Härdle, W., P. Hall, H. Ichimura, et al. (1993). Optimal smoothing in single-index models. *The annals of Statistics* 21(1), 157–178.

Hristache, M., A. Juditsky, and V. Spokoiny (2001). Direct estimation of the index coefficient in a single-index model. *Annals of Statistics* 29(3), 595–623.

Hutchinson, G. E. (1961). The paradox of the plankton. *The American Naturalist* 95(882), 137–145.

Ichimura, H. (1993). Semiparametric least squares (sls) and weighted sls estimation of single-index models. *Journal of Econometrics* 58(1-2), 71–120.

Koops, D. N., C. J. E. Metcalf, and S. Tuljapurkar (2008). Evolution of delayed reproduction in uncertain environments: a life-history perspective. *The American Naturalist* 172(6), 797–805.

Koops, D. N., S. Pavard, A. Baudisch, J. E. Metcalf, et al. (2009). Is life-history buffering or lability adaptive in stochastic environments? *Oikos* 118(7), 972–980.

Lewontin, R. C. and D. Cohen (1969). On population growth in a randomly varying environment. *Proceedings of the National Academy of Sciences* 62(4), 1056–1060.

Li, K.-C. (1991). Sliced inverse regression for dimension reduction. *Journal of the American Statistical Association* 86(414), 316–327.

Ma, S. (2016). Estimation and inference in functional single-index models. *Annals of the Institute of Statistical Mathematics* 68(1), 181–208.

Marron, J. and J. T. Zhang (2005). Sizer for smoothing splines. *Computational Statistics* 20(3), 481–502.

Ramsay, J. O. (2006). *Functional data analysis*. Wiley Online Library.

Ramsay, J. O., G. Hooker, and S. Graves (2009). *Functional data analysis with R and MATLAB*. Springer Science & Business Media.

Ruppert, D., M. P. Wand, and R. J. Carroll (2003). *Semiparametric regression*. Cambridge university press.

Teller, B. J., P. B. Adler, C. B. Edwards, G. Hooker, and S. P. Ellner (2016). Linking demography with drivers: climate and competition. *Methods in Ecology and Evolution* 7(2), 171–183.

Vasseur, D. A. and K. S. McCann (2007). *The Impact of Environmental Variability on Ecological Systems*. Springer Netherlands.

Wood, S. N. (2000). Modelling and smoothing parameter estimation with multiple quadratic penalties. *Journal of the Royal Statistical Society: Series B (Statistical Methodology)* 62(2), 413–428.

Ye, Z. and G. Hooker (2018). Local quadratic estimation of the curvature in a functional single index model. *arXiv preprint arXiv:1803.09321*.

A Plots of Estimated Curvature

This section provides plots provide examples of the accuracy of estimating a second derivative in a functional single index model. In each we plot the true and estimated link function and its second derivative. We also plot our estimated functional single index values versus their truth and the distortion that produces for the estimated second derivative.

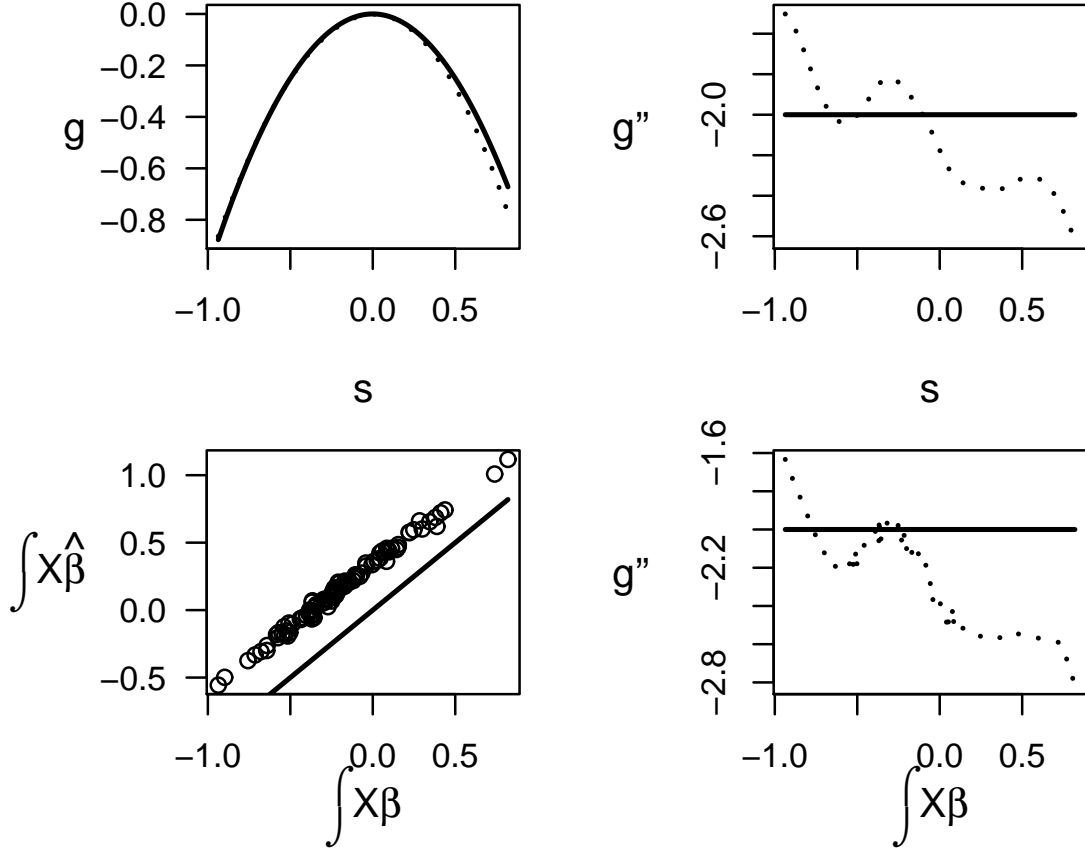


Figure 6: The link function is $g(s) = -s^2$. The top-left and right panel are the plots of g and g'' over 1000 equally-spaced grid points, while the lower and upper bound are the minimum and maximum of $\int X(t) \hat{\beta}(t) dt$. The bottom-right panel is the plot of g'' over the true $\int X(t) \beta(t) dt$. The black line is the true curve, while the red line is the estimated curve. The bottom-left panel is the plot of $\int X(t) \hat{\beta}(t) dt$ versus $\int X(t) \beta(t) dt$, while the red line is $y = x$.

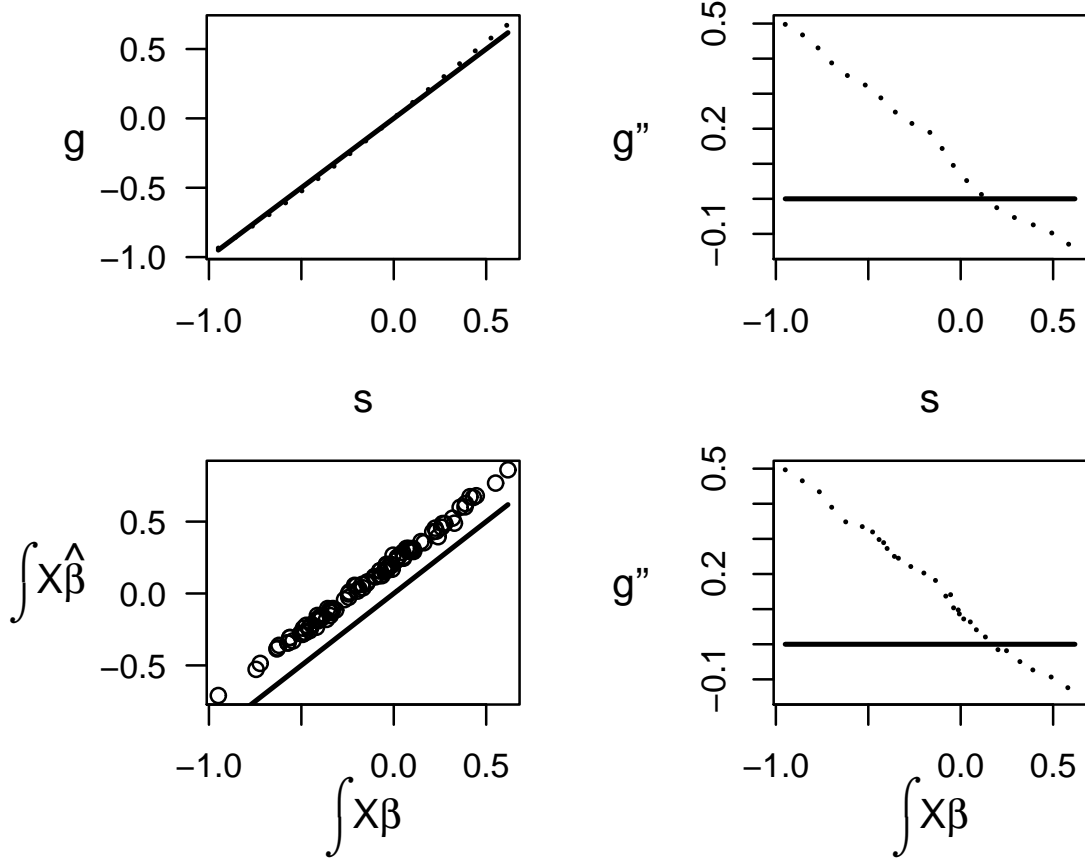


Figure 7: The link function is $g(s) = s$. The top-left and right panel are the plots of g and g'' over 1000 equally-spaced grid points, while the lower and upper bound are the minimum and maximum of $\int X(t) \hat{\beta}(t) dt$. The bottom-right panel is the plot of g'' over the true $\int X(t) \beta(t) dt$. The black line is the true curve, while the red line is the estimated curve. The bottom-left panel is the plot of $\int X(t) \hat{\beta}(t) dt$ versus $\int X(t) \beta(t) dt$, while the red line is $y = x$.

B Diagnostic Plots for the Jensen Effect: Single Index Model

These plots give example δ functions using a single index model and the corresponding t functions for links $g(s) = -s^2$ and $g(s) = s$ respectively.

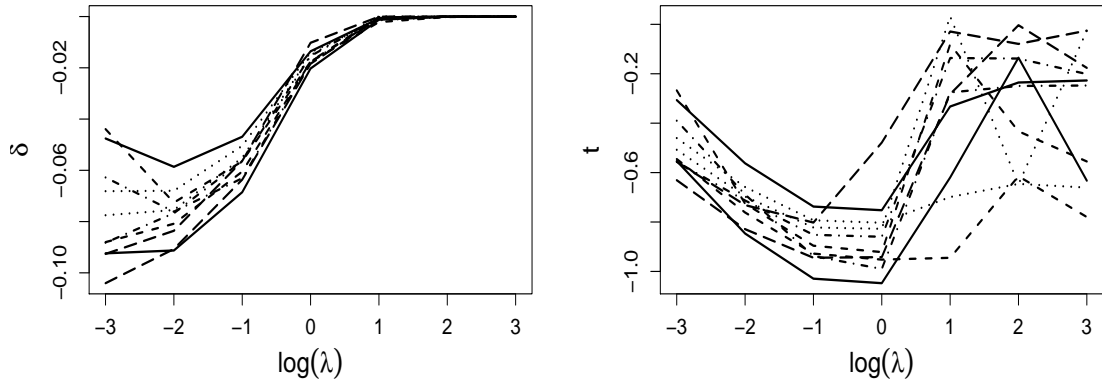


Figure 8: Left: a sample of δ_λ as a function of λ in a single index model with link function $g(s) = -s^2$. Right: the corresponding t_λ functions.

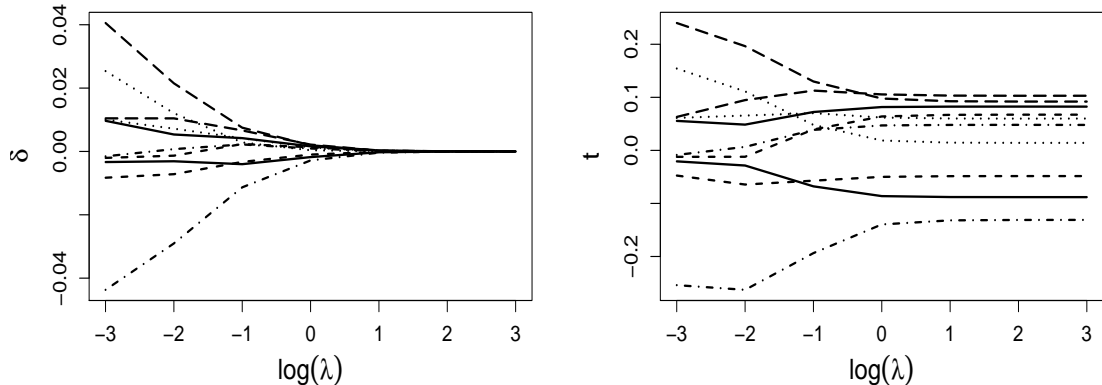


Figure 9: Left: a sample of δ_λ as a function of λ in a single index model with link function $g(s) = s$. Right: the corresponding t_λ functions.

C Diagnostic Plots for the Functional Single Index Model

These plots give example δ functions using a single index model and the corresponding t functions for links $g(s) = -s^2$ and $g(s) = s$ respectively.

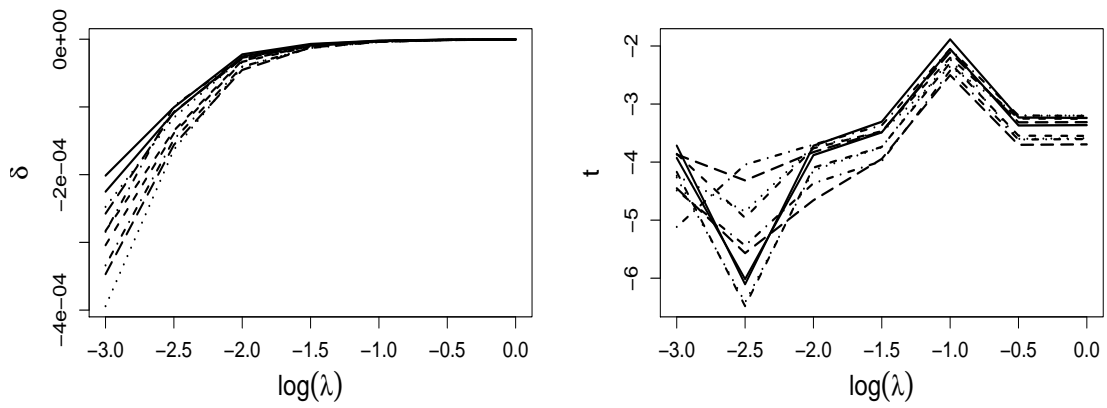


Figure 10: Left: a sample of δ_λ as a function of λ in a functional single index model with link function $g(s) = -s^2$. Right: the corresponding t_λ functions.

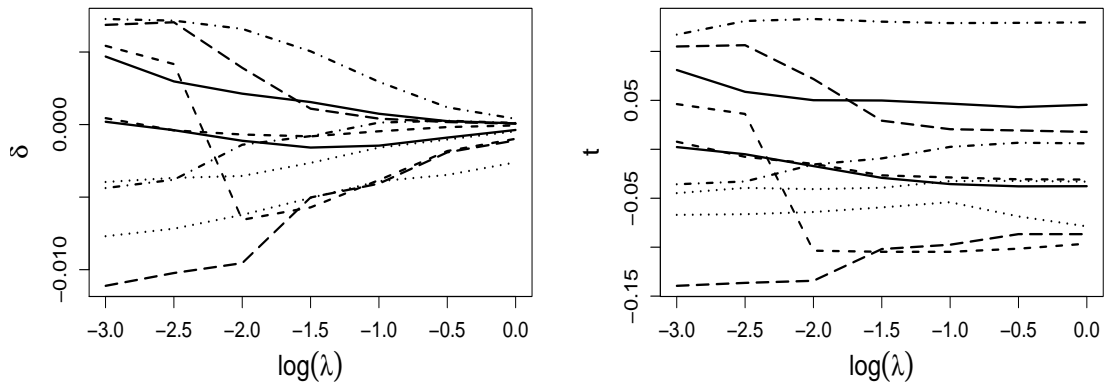


Figure 11: Left: a sample of δ_λ as a function of λ in a functional single index model with link function $g(s) = s$. Right: the corresponding t_λ functions.

D Plots for the copepod data

Plots 12 through 20 provide descriptive plots for each species from the copepod study. We provide a plot of δ versus $\log(\lambda)$ with the value selected by GCV in red. We also provide plots of $\hat{\beta}$, \hat{g} and \hat{g}'' at the value of λ selected by GCV along with approximate pointwise confidence intervals.

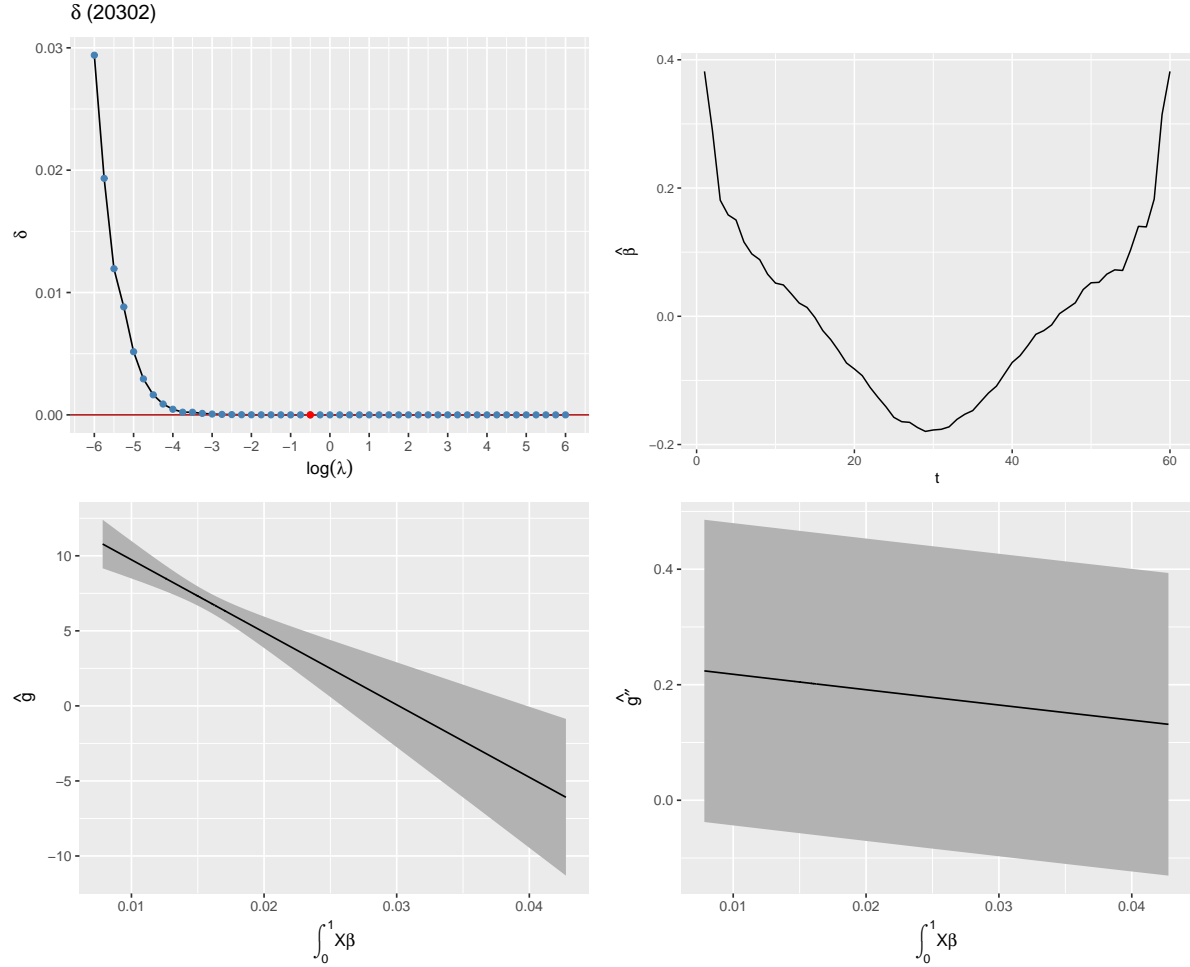


Figure 12: Plots for *Diacyclops Thomasi*.

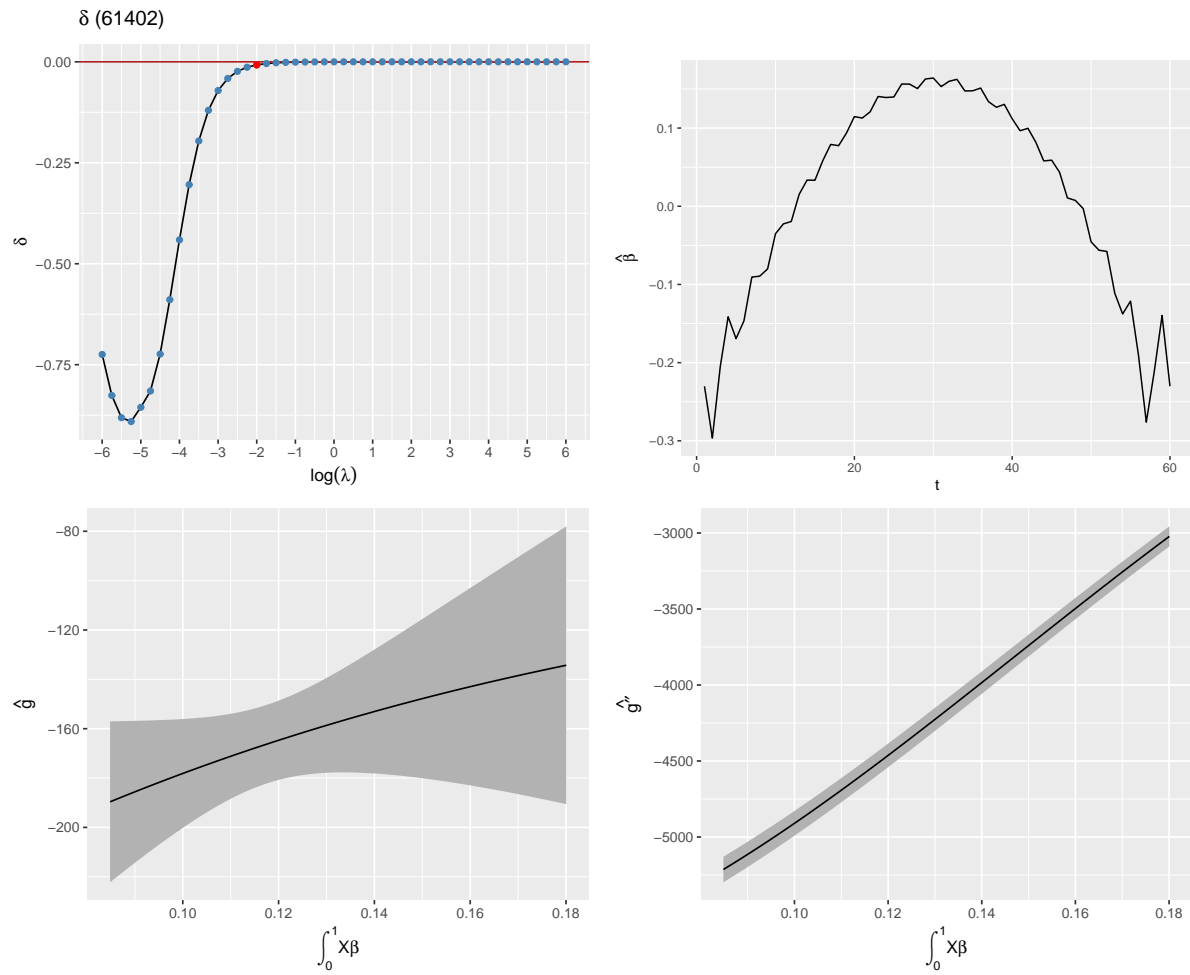


Figure 13: Plots for *Filinia Terminalis*.

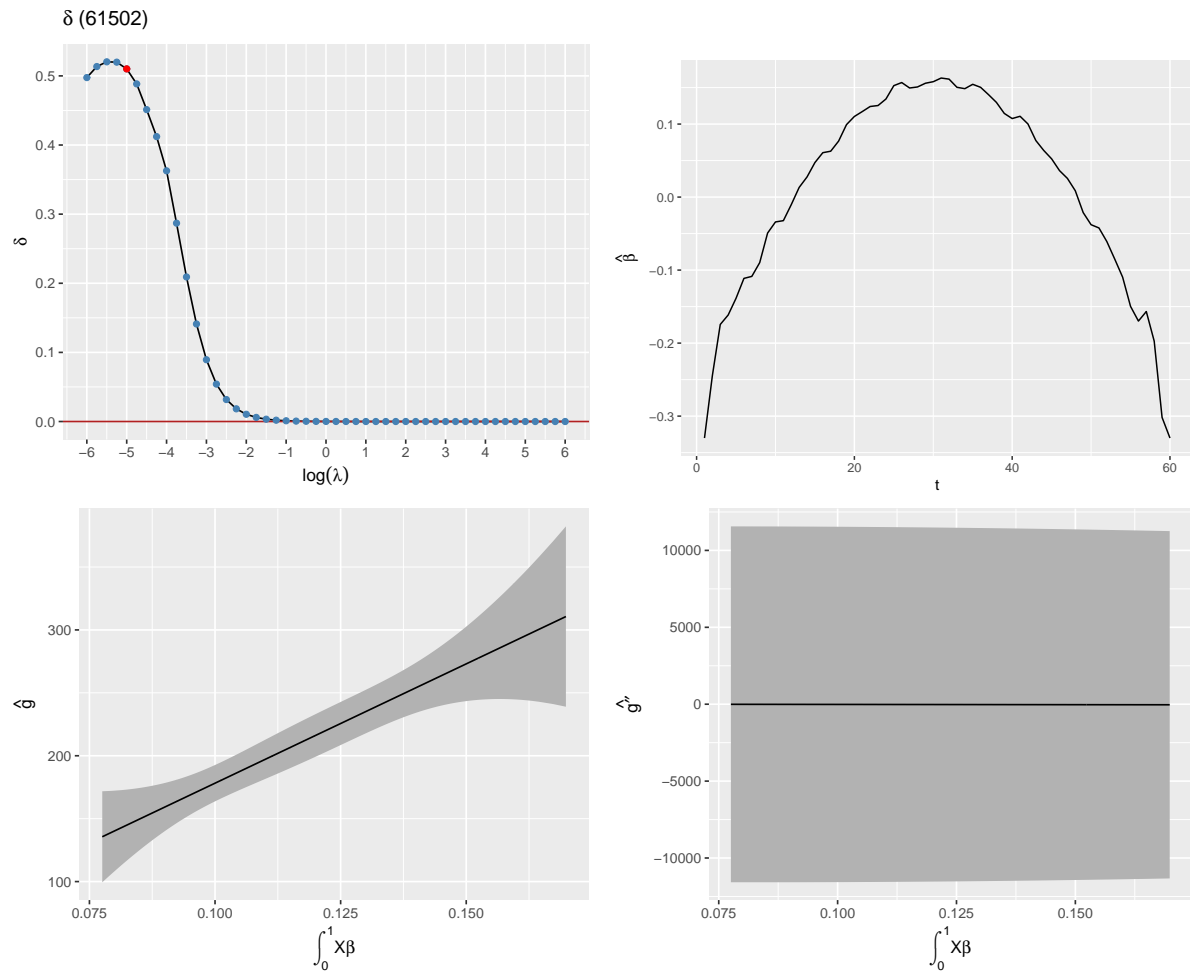


Figure 14: Plots for *Gastropus Stylifer*.

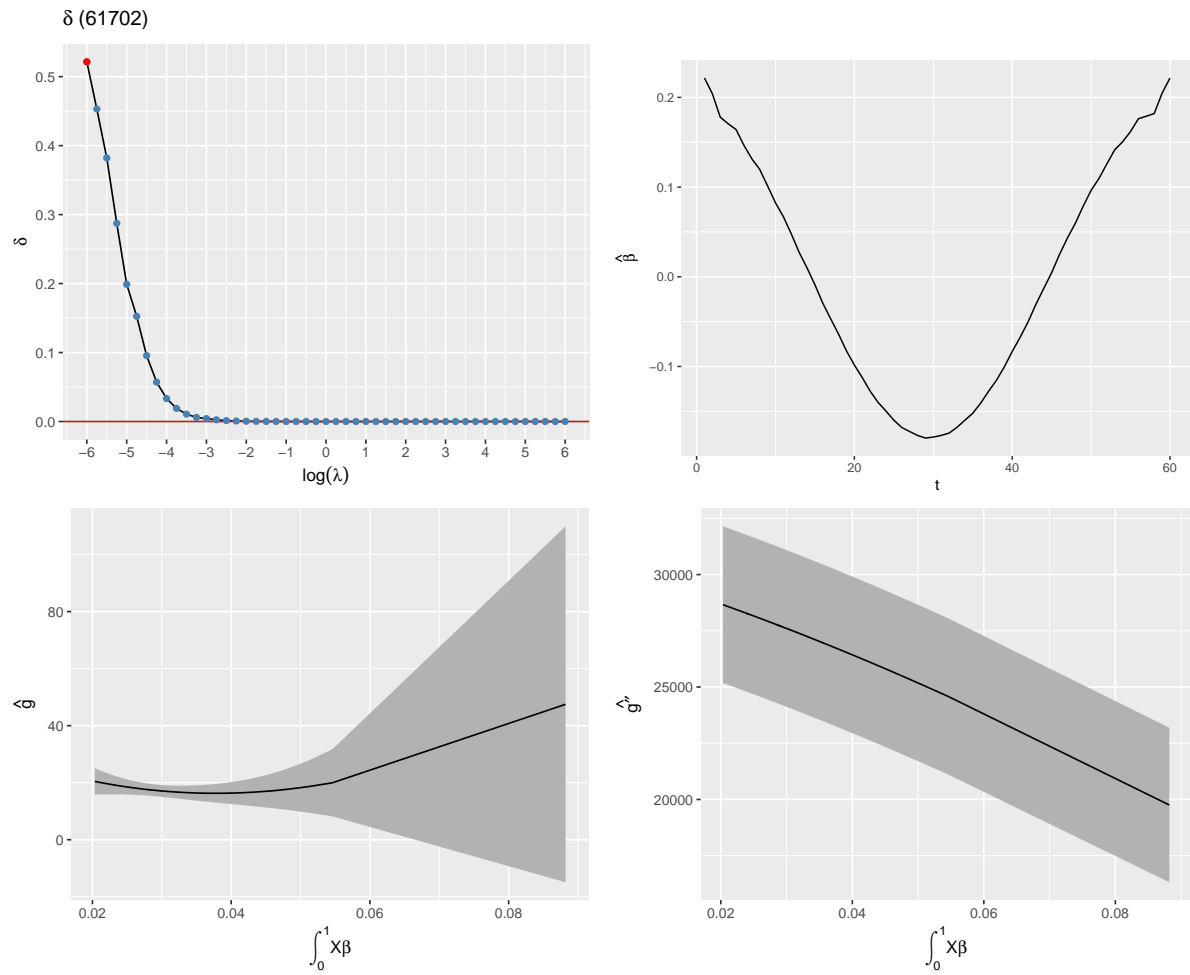


Figure 15: Plots for *Kellicottia Longispina*.

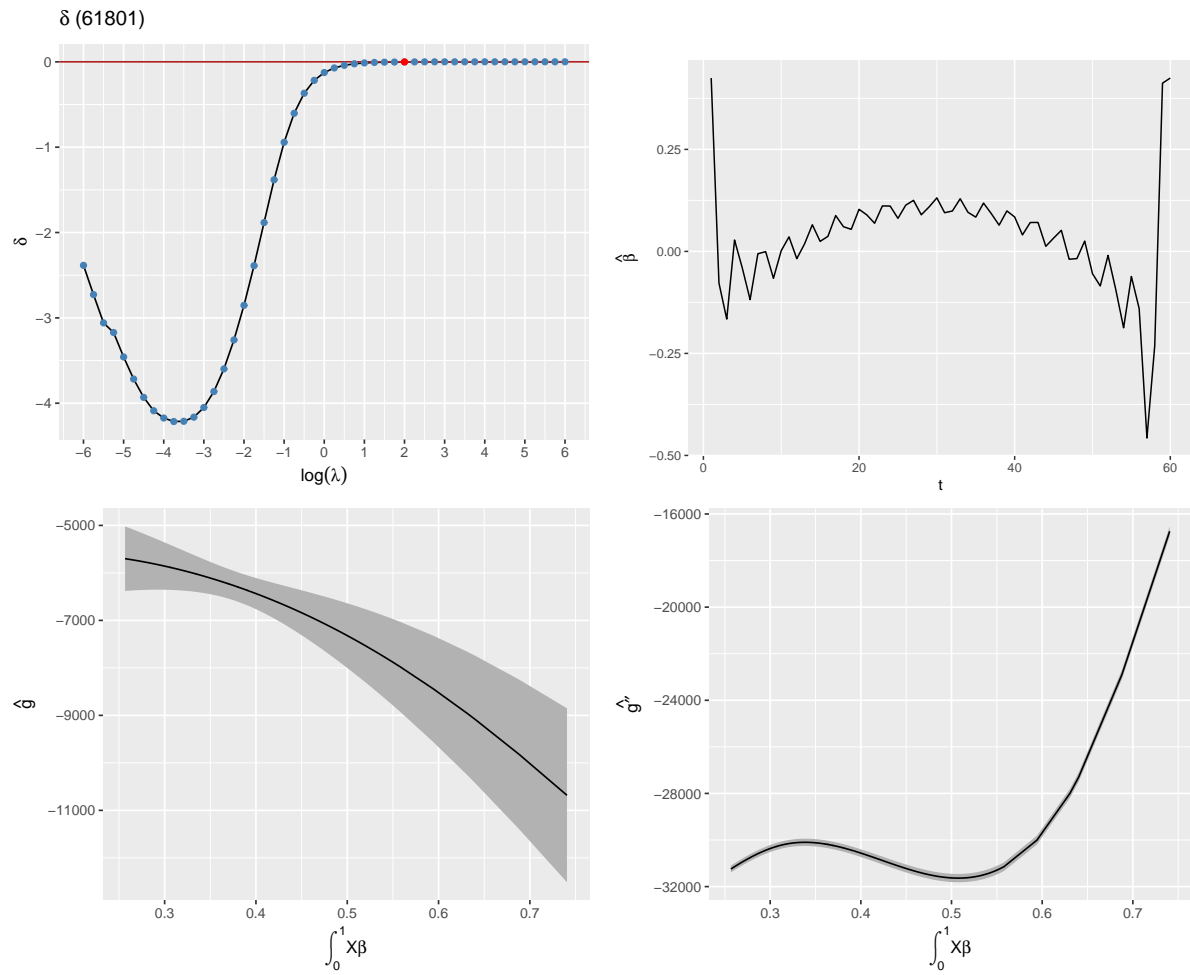


Figure 16: Plot for *Keratella Cochlearis*.

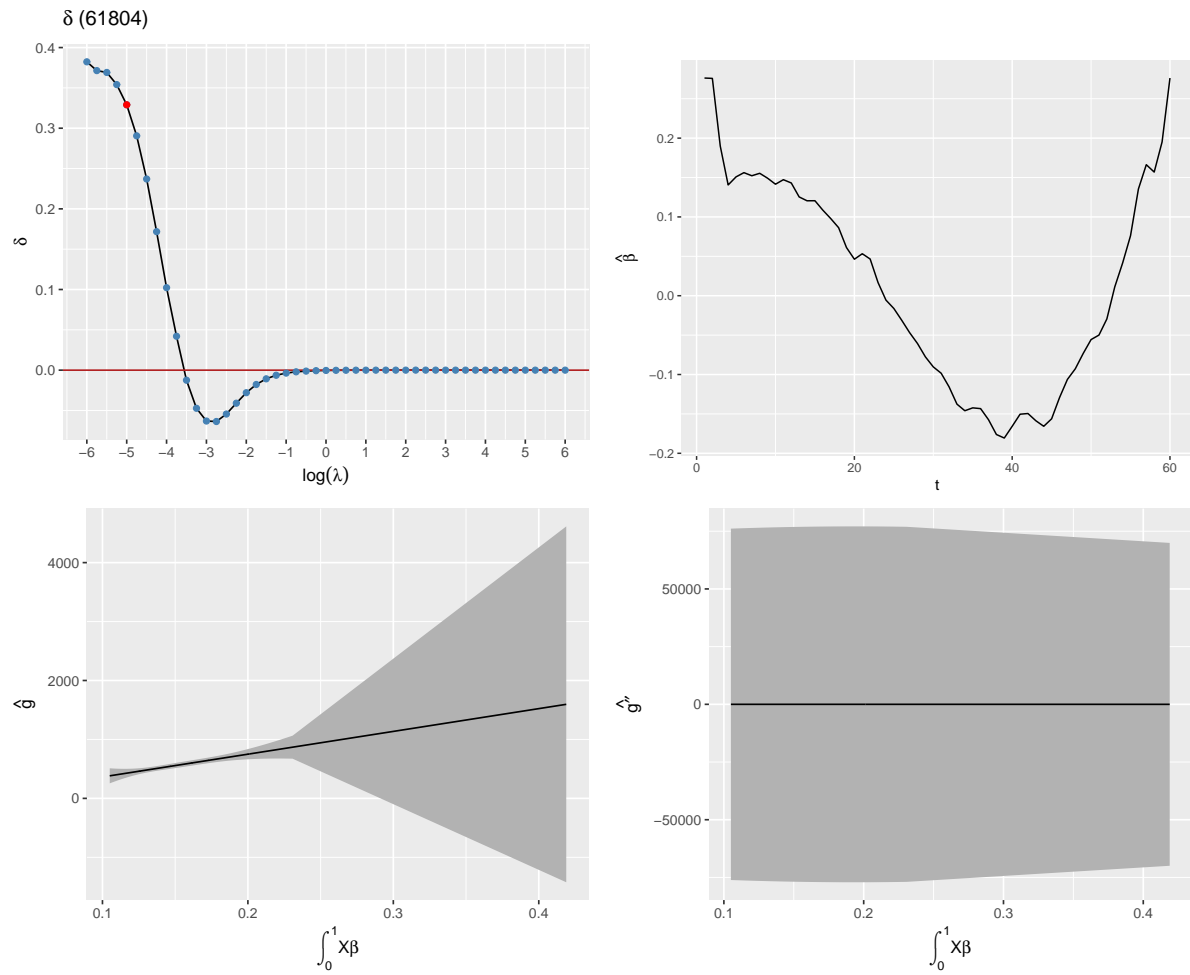


Figure 17: Plot for *Keratella Earlinae*.

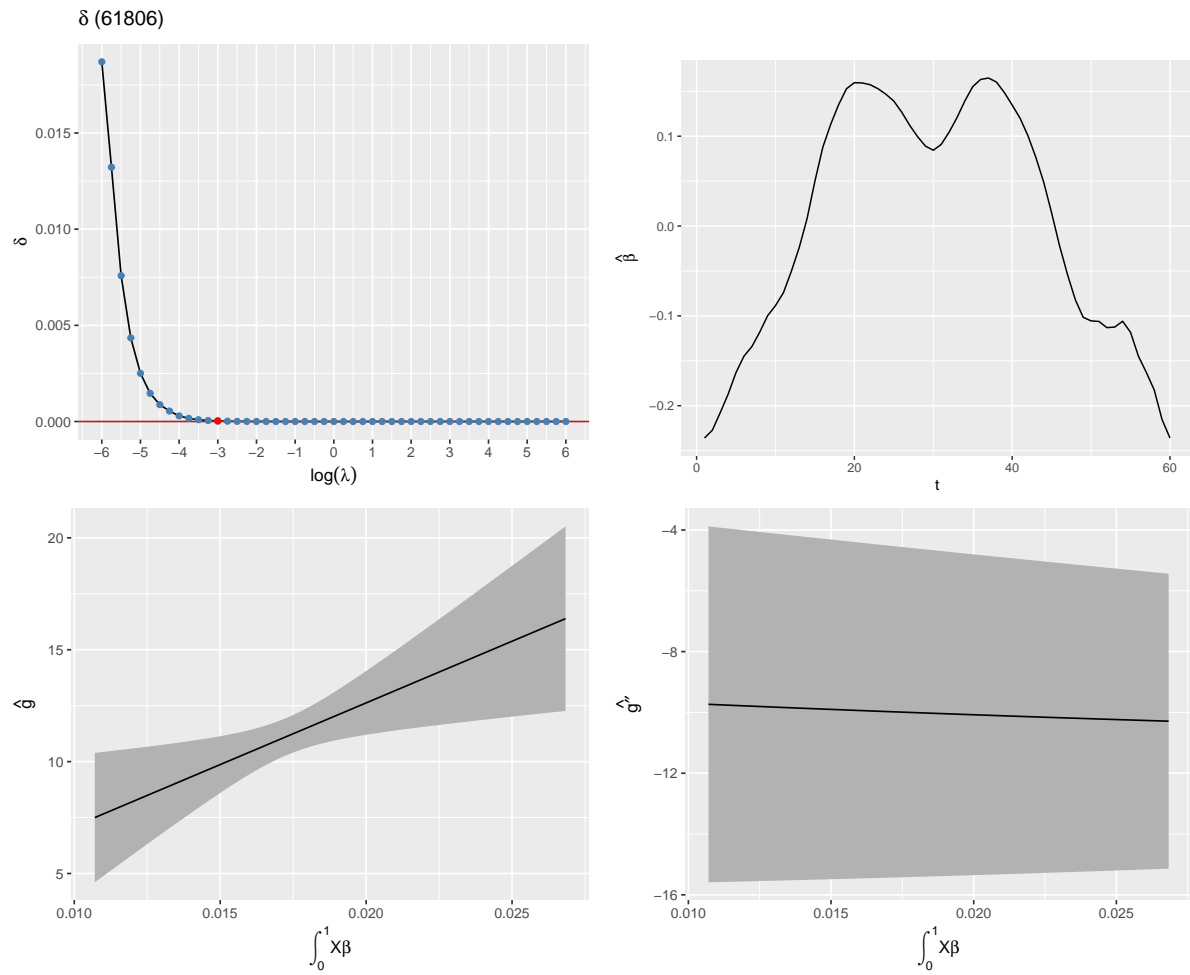


Figure 18: Plot for *Keratella Quadrata*.

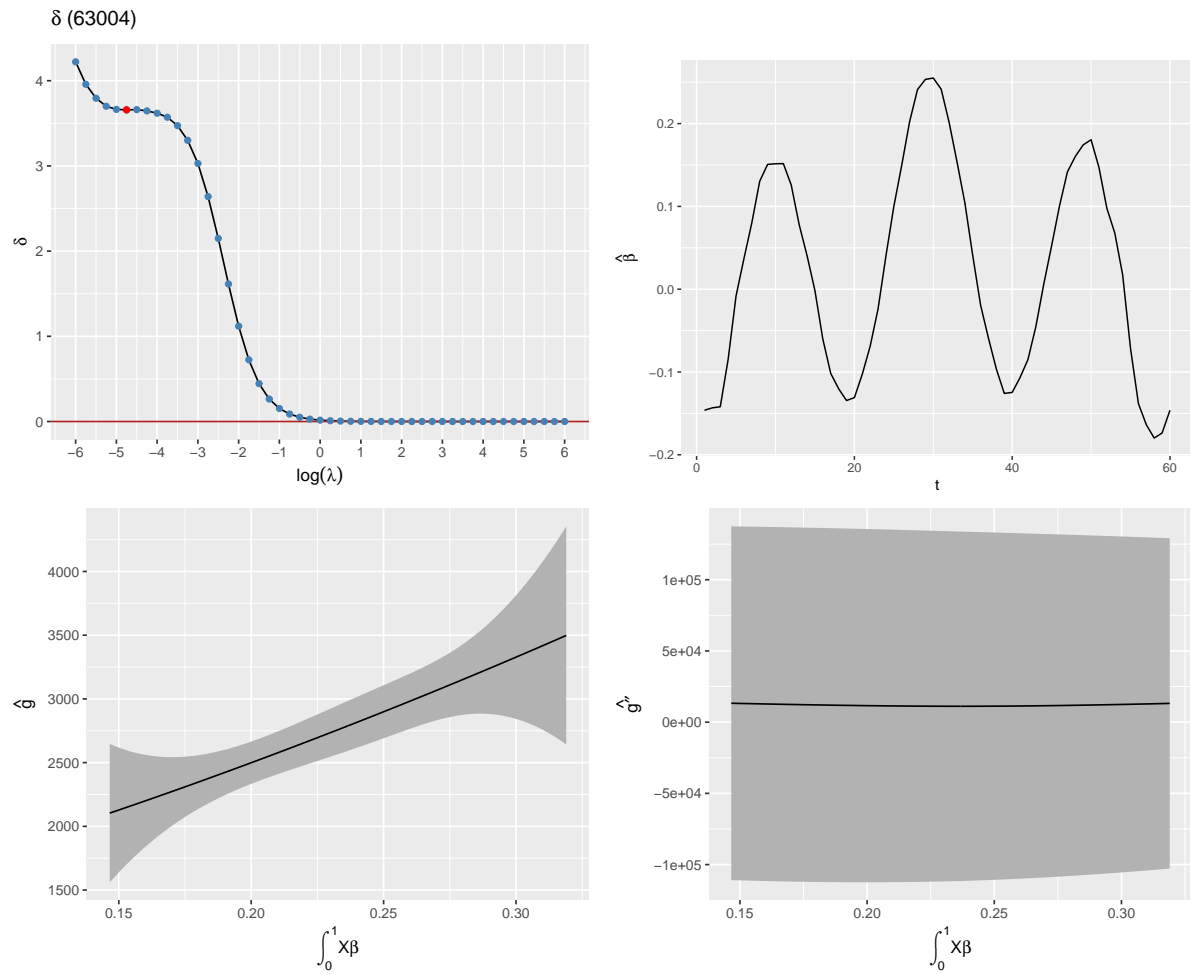


Figure 19: Plot for *Polyarthra Remata*.

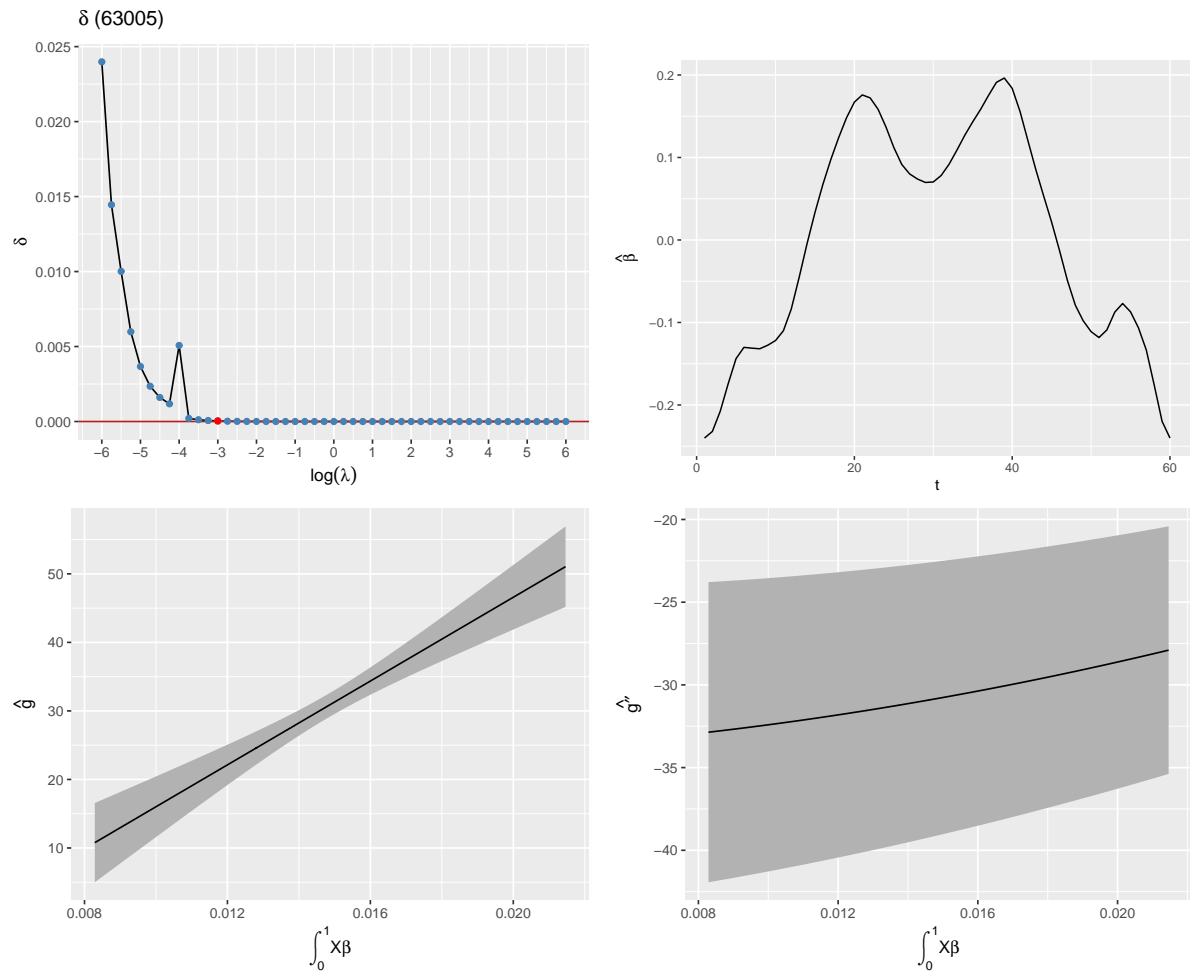


Figure 20: Plot for *Polyarthra Vulgaris*.